



# Investigation of dual-band bandpass filter inspired by a pair of square coupled interlinked asymmetric tapered metamaterial resonator for X-band microwave applications

AHMED YACINE ROUABHI<sup>1</sup>, MOHAMMED BERKA<sup>1,2,\*</sup> , AMINA BENADAUDI<sup>1</sup>  
and ZOUBIR MAHDJOUR<sup>1</sup>

<sup>1</sup>EPO Laboratory, Electronic Department, Sidi Bel Abbès University, 22000 Sidi Bel Abbès, Algeria

<sup>2</sup>Electrical Engineering Department, Science and Technology Faculty, Mustapha Stambouli University of Mascara, 29000 Mascara, Algeria

\*Author for correspondence (m.barka@univ-mascara.dz)

MS received 10 November 2021; accepted 12 February 2022

**Abstract.** Advanced studies on modern electronic devices using the filter function show the impact of multi-band filters on the electrical qualities of these devices. Due to the importance of its electromagnetic characteristics, the dual-band bandpass microwave filters can be used in several high-quality electronic devices. In this paper, a dual-band bandpass filter (DBBPF) is provided. The proposed filter is inspired by a pair of tapered split-ring metamaterial resonators of the same asymmetric square coupled interlinked shape (SCI-SRR) and of different sizes. The choice of the two resonators, which have a negative permeability ( $\mu < 0$ ), is made such that the magnetic resonance of each resonator appears in X-band. The designed filter consisting of these SCI-SRRs is fed in parallel mode by two microstrip lines and etched on the upper face of the used substrate. Both SCI-SRRs which are coupled to the feed lines are interconnected by a folded microstrip line to have the necessary miniaturization of the filter. The electrical dimensions of our DBBPF are  $(1.305 \lambda_0 \times 0.913 \lambda_0)$  mm<sup>2</sup>, for which  $\lambda_0$  is the wavelength of the lowest frequency calculated at 9.89 GHz. Numerical calculations using the finite element method (FEM) based on high-frequency structure simulator software are performed to design this filter. The two filter bandwidths, which are obtained as a function of the rings widths of the tapered metamaterial resonators ( $\alpha, \beta$ ), are considered in the X-band, they are of the order of 186.2 and 89.7 MHz, respectively. To validate our work, we compared our obtained results with the other recent work results for the same field of research.

**Keywords.** Bandpass filter; metamaterial; permeability; SCI-RRs; taper.

## 1. Introduction

For nearly a century, the filtering function is still an important function for the development of modern electronic devices. The weight and the size problem of the filter structures require the integration of several components in a small area. Today, multi-band filters [1–4] can help us to avoid the use of several filtering devices in the same area. Because of its electrical qualities, the dual-band bandpass microwave filter (DBBPF) can offer several advantages and solve several problems (sizes and losses) for electronic systems operating at microwave frequencies [5–7]. Therefore, optimization of the DBBPF appears to be one of the most desired goals.

The trend towards miniaturized filters can cause several problems during the design and also during the realization. So, the increase of losses in such a filter is still one of the most undesirable phenomena. Several solutions have been proposed to design miniaturized multi-band filters with less loss, the choice of design materials represents one of the

most effective solutions. In the last two decades, an unusual class of materials can meet the majority of these needs; this class is called Metamaterials.

The concept of metamaterial was started for the first time (theoretical studies only) with the suggestion of the Russian physicist Victor Veselago in 1967 [8]. With their studies, Veselago presented general properties of the propagation of electromagnetic waves in this type of medium. He showed the unusual properties of metamaterials that are not found in nature. Later, Smith and his research group suggested a new type of metamaterial that simultaneously offers negative permittivity and permeability [9–12]. The common point between most of these researches is to obtain resonators of magnetic activity capable of providing negative permeability; this is the main objective of the famous Sir John Pendry [13]. The platform dedicated by Pendry to this field allowed to define a new type of resonator now called Split Ring Resonator abbreviated as SRR.

In the fundamentals of metamaterial resonators, the SRR is formed by two inner and outer rings. The geometric shape

of the two rings and their dimensions can make the difference between one metamaterial resonator and the other. Several geometric shapes have been proposed and studied by the designers. Altıntaş *et al* [14] designed an omega-shaped metamaterial resonator with millimetre dimensions for sensor applications. A (D-Z) shaped geometric is proposed for the design of a metamaterial resonator for L-, S- and X-band applications [15]. Berka *et al* [16] have designed a dual-bandpass filter based on a twin of ordinary square resonators and complementary symmetrical square resonators. A double L-shaped metamaterial resonator has been realized for C-, X- and Ku-band applications [17]. Rajkumar and Kommuri [18] presented an analysis of a microwave antenna based on a triangular-shaped metamaterial resonator for multiband operations. In terms of dimensions, two major classes of split-ring metamaterial resonators may be intervening in the various electronic devices; ordinary resonators (where the width of the rings is the same) and the tapered resonators (where the width of the two rings is narrowed from one region to the other). Tapered SRRs can offer several advantages over ordinary SRRs, but the most interesting is the possibility of having improved magnetic resonance over a wide bandwidth [19].

In this paper, we provide a dual-band bandpass microwave filter inspired by two tapered metamaterial split-ring resonators for the asymmetric square coupled interlinked shaped SCI-SRRs and for two different sizes. The dimensions of the two SCI-SRRs are chosen to have a magnetic resonance located in the X-band. Our design approach is based on exploiting the electromagnetic qualities of the tapered shape for each resonator and also based on the electromagnetic coupling between the two SCI-SRRs forming the filter and the two feed-lines.

## 2. Design approach

### 2.1 Description of SCI-SRR

The electrical circuit representation of a metamaterial tapered resonator shows that it is generally constituted by an inductance ( $L$ ) and a capacitance ( $C$ ). From the numerical values of these two components ( $L$  and  $C$ ), the magnetic resonance of such a resonator can be calculated. The physical dimensions of the tapered resonator that are not homogeneous (by all the sides) can increase the equivalent inductance and capacitance.

Metamaterial resonators can be studied for too small wavelengths ( $\lambda \ll \lambda$ ). The frequency response of such a basic cell will be more efficient for sizes relatively smaller than that of  $\lambda$  [20]. The choice of dimensions for the metamaterial structures is made according to the desired resonance of the structure itself. For our design, we want a basic cell that should resonate in the X-band. For this reason, the wavelength will be 37.5 mm for the lowest frequency of the band, which is 8 GHz. We will choose three

(03) period  $P$  for our basic cell ( $P = 8$  mm,  $P = 10$  mm and  $P = 12$  mm). So, the longest period chosen among the three will be closer to the quarter-wave ( $P \approx \lambda/4$ ). The proposed unit cell structure is derived from the split-ring resonator in a modified form. This structure is made up of two internal and external rings for the square tapered shape, with two gaps (equal in their widths) for each one. A tapered arm on these two sides is placed between the two branches forming the internal ring to interconnect them. The inner and outer rings are coupled together at inter-resonator spacing. The set of two rings and the tapered arm form our proposed metamaterial resonator. The proposed SCI-SRRs resonate correctly when the magnetic field is perpendicular to the plane of the two rings. The problem of symmetry appears when we want to polarize the resonator, while for the two rings constituting our SCI-SRR, we have no symmetry. The diagram of the prospective structure is shown in figure 1.

The magnetic resonance of our SCI-SRR is influenced by the proposed dimensions and also by the material of the chosen substrate. Our parametric study is based on the study of three SCI-SRRs of different sizes. The proposed dimensions for the three SCI-SRRs are varied according to  $(\alpha, \beta)$  parameters, with

$$\begin{cases} w_2 = \alpha w_1 \\ w_3 = \beta w_1 \end{cases} \quad (1)$$

where  $w_1, w_2, w_3$  represents the widths of the three arms of the asymmetrical rings of each SCI-SRR of period  $P$  to obtain the tapered shape. For each resonator we have ( $e = s = g = S = 0.2$  mm) and ( $w_1 = 0.1$  mm,  $d = 0.4$  mm). The dimensions of the three SCI-SRR are summarized in table 1.

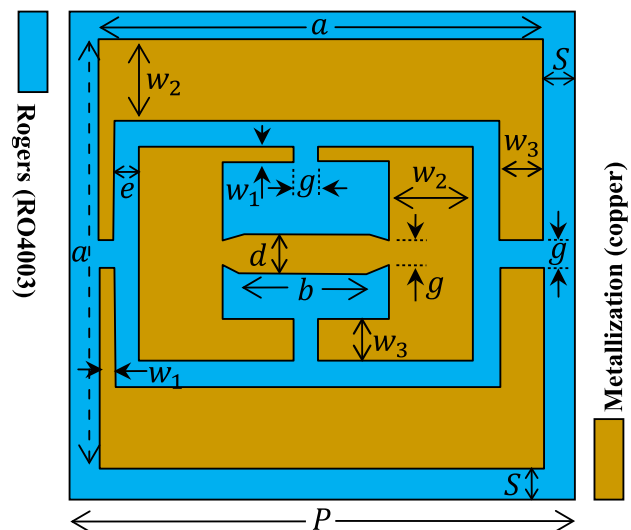


**Figure 1.** Representation in rings of the proposed SCI-SRR.

**Table 1.** Dimensions of the SCI-SRR for different  $(\alpha, \beta)$ .

	Parameter	$a$	$b$	$P$
Values (mm)	(SCI-SRR) <sub>1</sub> ( $\alpha = 4, \beta = 2$ )	7.6	5.9	8
	(SCI-SRR) <sub>2</sub> ( $\alpha = 6, \beta = 4$ )	9.6	7.3	10
	(SCI-SRR) <sub>3</sub> ( $\alpha = 10, \beta = 6$ )	11.6	8.3	12

2.2 A proposed DBBPF

The overall filter is formed by two metamaterial resonators (SCI-SRRs) among the three resonators previously proposed for the study. We have chosen the resonators (SCI-SRR)<sub>3</sub> and (SCI-SRR)<sub>2</sub> that have the largest and medium areas, respectively. These two resonators are parallelly fed by two microstrip lines of the same width ( $W$ ) and of different lengths (because of the two different sizes of the two chosen resonators); the input line is length ( $l_{in}$ ) and the output line is length ( $l_{out}$ ). The two SCI-SRRs forming the global filter are interconnected together by a folded arm (to have the necessary miniaturization) of width ( $W_r = W$ ) and length ( $2l_r + L$ ). This arm is coupled to the two feed-lines by a ( $e_p$ ) spacing. Our global filter has the area ( $m \times n$ ) mm<sup>2</sup>, where,

$$\begin{cases} m = l_{in} + l_{out} + 2e_p + W_r \\ n = 2S_F + L + W + \frac{1}{2}(a_3 + a_2) \end{cases} \quad (2)$$

The configuration of the proposed DBBPF is represented in figure 2.

With,

$$\begin{cases} l_{in} = a_2 + S_F + l_r - (W_r + e_p) \\ l_{out} = a_3 + S_F + l_r - (W_r + e_p) \end{cases} \quad (3)$$

and,

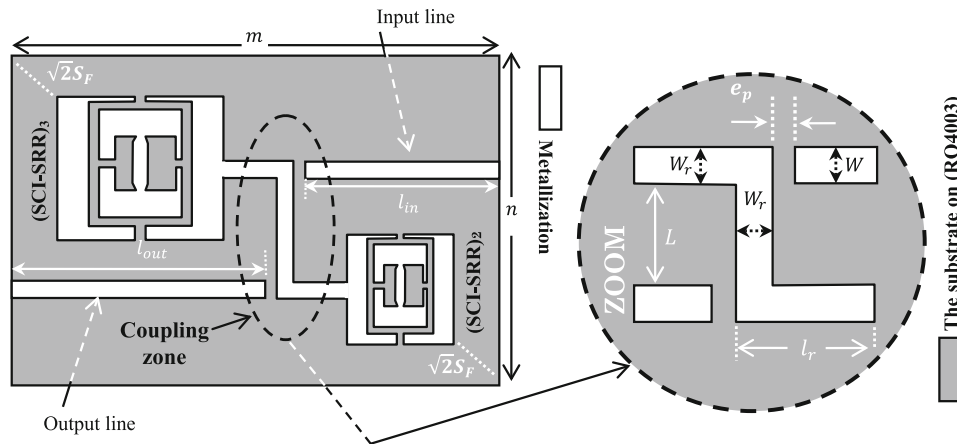


**Figure 2.** Proposed DBBPF configuration.

$$\begin{cases} a_3 = a|_{\alpha=10, \beta=6} \\ a_2 = a|_{\alpha=6, \beta=4} \end{cases} \quad (4)$$

The global filter is etched on the same chosen substrate, which is the RO4003.

3. Results and discussion

3.1 Electromagnetic characteristics of SCI-SRR

In planar technology, a good choice of dielectric substrate can improve the electrical qualities of microwave devices. The choice of such a substrate is generally made according to two criteria; losses and absorption coefficients. Depending on the nature of the microwave structure desired, we can choose a suitable substrate for the design. A study of the physical characteristics of three (03) types of dielectric substrates is made by Berka *et al* [6]. According to the obtained results, the Rogers (RO4003) represents the least absorber substrate, which meets the requirements of metamaterial filters. RO4003 is an available substrate that has a relative permittivity of 3.55 and a dielectric loss tangent of 0.0027. We will use this type of substrate for a thickness  $h = 0.85$  mm. The SCI-SRR of each proposed period must be engraved for a thickness  $t = 0.015$  mm. The simulation model for one of the three squares SCI-SRRs ((SCI-SRR)<sub>3</sub> in table 1; whose  $P_3 = 12$  mm for  $\alpha = 10, \beta = 6$ ) is shown in 3-D Modeler of the high-frequency structure simulator (HFSS), as shown in figure 3.

We have introduced the necessary band conditions which are fixed according to the electromagnetic field ( $E$  and  $H$ ) propagating in our resonator. Therefore, the electric field must be perpendicular to the gap of the outer ring of the resonator on the two surfaces of the ray box (PEC1 and PEC2). The magnetic field must be perpendicular to the plane of the two rings constituting the resonator (PMC1 and PMC2) and the two wave ports are maintained in such a

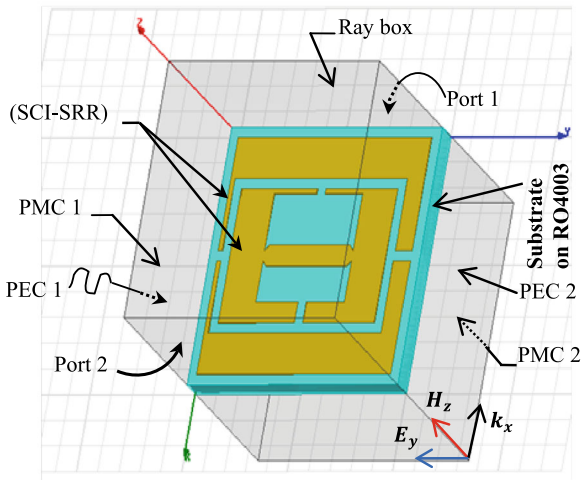


**Figure 3.** Simulation model of the (SCI-SRR)<sub>3</sub>.

way that  $\mathbf{k} \perp \mathbf{E}$  and  $\mathbf{k} \perp \mathbf{H}$ , as shown in figure 3. After having applied all these criteria, the reflection and the transmission coefficients of the three SCI-SRRs are shown in figure 4.

Figure 4 shows the dimensions parameter effect on the characteristics of our metamaterial resonators. The reflection and transmission coefficients of the three SCI-SRRs are represented over the 5–15 GHz frequency range. Note that the behaviour of each studied metamaterial resonator is band-stop; the resonance of each SCI-SRR is obtained according to its dimensions. For the smallest period, we will have the most important magnetic resonance and vice versa. So, for  $P_1 = 8$  mm, the resonance is 12.70 GHz with a maximum attenuation of  $-23.14$  dB, for  $P_2 = 10$  mm the resonance is 10.86 GHz with a maximum attenuation of  $-26.92$  dB and for  $P_3 = 12$  mm; the resonance is 10.12 GHz with a maximum attenuation of  $-16.24$  dB. According to these three frequency characteristics, it is noted that the two resonators, the largest and the middle resonate in the X-band, but the smallest one resonates outside this frequency band. The two reflection and transmission coefficients of the middle resonator (SCI-SRR)<sub>2</sub> (relative to the other two resonators) are shown in figure 4c. It is observed that the stop-band behaviour begins at about 7.93 GHz; the rejection band is of the order of 1.01 GHz. For the two other resonators (SCI-SRR)<sub>1</sub> and (SCI-SRR)<sub>3</sub>, the stop frequencies are observed at 10.78 and 13.37 GHz, respectively.

For the resonator (SCI-SRR)<sub>3</sub> which is represented in figure 3 such as  $P_3 = 12$  mm and  $(\alpha = 10, \beta = 6)$ , we will present the characteristics of the permeability ( $\mu_{\text{eff}}$ ) and the refractive index ( $n_{\text{eff}}$ ). Nicolson-Ross-Weir (NRW) method [21,22] is very popular for extracting this kind of effective parameter. The information obtained from HFSS related to the reflection coefficient  $|S_{11}|$  and transmission coefficient  $|S_{21}|$  can be used in NRW approach to extract these parameter values. In this approach, two composite terms  $V_1$

and  $V_2$  are initiated by the subtraction and addition of  $[S]$  parameter values [23,24].

The effective permeability of the (SCI-SRR)<sub>3</sub> resonator is given by the following expressions.

$$\mu_{\text{eff}}(f) = \frac{2}{jkh} \left( \frac{1 - V_1}{1 + V_1} \right) \quad (5)$$

In which,

$$V_1 = |S_{21}| - |S_{11}| \quad (6)$$

and  $k$  is the wavenumber, it is equal to  $\omega/c_0$  ( $\omega$  is the frequency in  $\text{rad s}^{-1}$ ) and  $c_0$  is the speed of light,  $h$  is the thickness of the used substrate.

Hence, equation (5) becomes,

$$\mu_{\text{eff}}(f) = \mu'_{\text{eff}} - j\mu''_{\text{eff}} = \frac{2}{jkh} \left[ \frac{1 - |S_{21}| + |S_{11}|}{1 + |S_{21}| - |S_{11}|} \right] \quad (7)$$

On the simulator, both real and imaginary parts of the permeability are shown in figure 5.

The variation of the effective permeability of the proposed resonator (SCI-SRR)<sub>3</sub> is shown in figure 5. In this figure, we observe relatively low values for the imaginary part ( $\text{Im}\{\mu_{\text{eff}}\} \approx 0$ ), except around the magnetic resonance where we observe a peak of the order of 3.2. Around the same resonance, we notice that the characteristic  $\text{Re}\{\mu_{\text{eff}}\}$  changes their sign; it was positive at the frequency of 10.37 GHz and becomes negative at 10.40 GHz. Then from this narrow band of the order of 30 MHz (where the band designating the left-hand behaviour is justified by the characteristic of the refractive index represented later), the resonator (SCI-SRR)<sub>3</sub> can offer its unusual properties for the design of our filter. The refractive index of the metamaterial resonator is related to its permittivity and its permeability; it is expressed by the following relation:

$$n_{\text{eff}}^2(f) = \mu_{\text{eff}}(f)\epsilon_{\text{eff}}(f) \quad (8)$$

with,

$$\epsilon_{\text{eff}}(f) = \frac{2}{jkh} \left( \frac{1 - V_2}{1 + V_2} \right) = \frac{2}{jkh} \left[ \frac{1 - |S_{21}| - |S_{11}|}{1 + |S_{21}| + |S_{11}|} \right] \quad (9)$$

and,

$$V_2 = |S_{21}| + |S_{11}| \quad (10)$$

The real and imaginary parts of the refractive index of the (SCI-SRR)<sub>3</sub> are shown in figure 6.

The frequency characteristic of the effective refractive index ( $n_{\text{eff}}$ ) of the resonator (SCI-SRR)<sub>3</sub> is shown in figure 6. At the frequency 10.4 GHz, the refractive index is a complex quantity that writes in the form  $-2.37 + i1.17$ . In the same figure, we observe a left-hand behaviour of the concerned resonator in the 10.26–11.87 GHz range. So for this range of length of 1.61 GHz, the losses which are manifested by the increases in the imaginary parts of  $n_{\text{eff}}$  can be minimized.

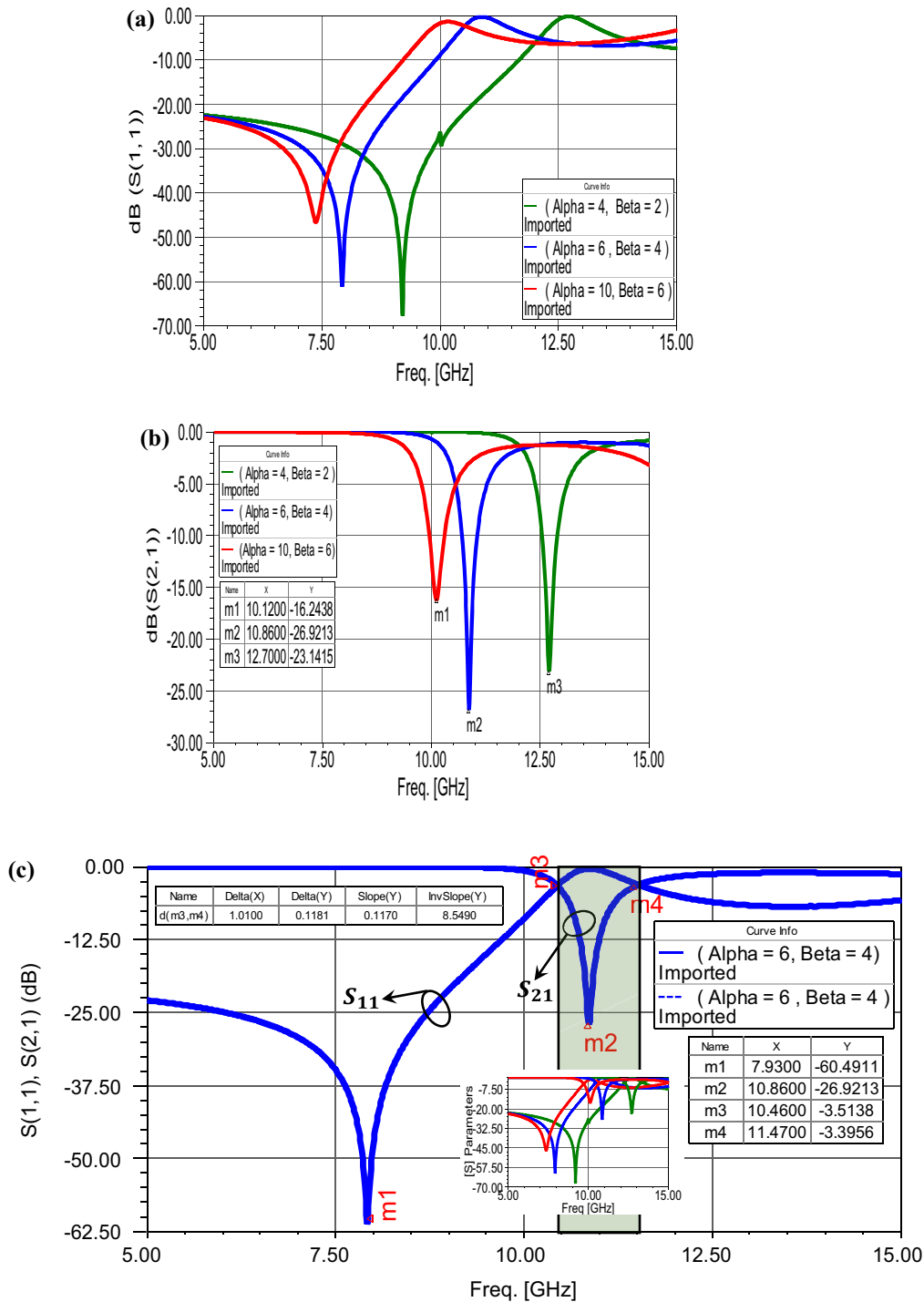


**Figure 4.** Behaviour of the three SCI-SRRs; **(a)** reflection coefficients, **(b)** transmission coefficients and **(c)** start and stop frequencies for middle resonator.

Another important parameter that can intervene during the study of metamaterial resonators in split rings is the Figure of Merit (FOM). This parameter can estimate the amount of losses in such a resonator and also it can judge the physical quality of the refractive index of each metamaterial resonator. Generally, the FOM is related to the real

and imaginary parts of the refractive index of the resonator by the relation below [25].

$$\text{FOM} = -\frac{\text{Re}(n_{\text{eff}})}{\text{Im}(n_{\text{eff}})} \tag{11}$$

This characteristic is illustrated in figure 7.

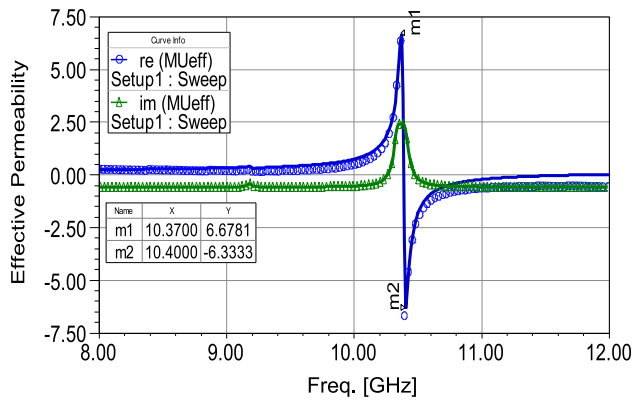


Figure 5. Permeability of the (SCI-SRR)<sub>3</sub>; real and imaginary parts.

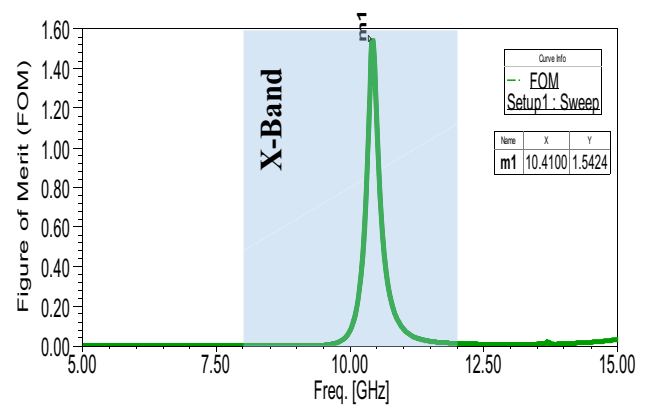


Figure 7. The figure of Merit (FOM) of the (SCI-SRR)<sub>3</sub>.

In figure 7, we note that the FOM of the third chosen resonator is resonated in the X-band, while a peak of maxima appears around the resonance, where we have exactly (FOM = 1.54) for the frequency 10.41 GHz. This maximum value of the FOM allows us to conclude that the (SCI-SRR)<sub>3</sub> resonator can contribute to the design of our filter or any other microwave device without correspondingly increasing the losses in these devices for the proposed dimensions.

### 3.2 Electrical qualities of the proposed filter

For the dimensions of our proposed filter, we have chosen ( $W_r = W = 0.6$  mm,  $L = 8.5$  mm,  $S_F = 4$  mm,  $e_p = 0.4$  mm and  $l_r = 5.5$  mm). The two feed lines at the input and output are  $l_{in} = 18.1$  mm,  $l_{out} = 20.1$  mm, respectively. The area (for physical dimensions) of our overall DBBPF becomes ( $m \times n$ ) = (39.6 × 27.7) mm<sup>2</sup>. The proposed DBBPF (for these dimensions) is shown on the 3-D Modeler of the HFSS in figure 8.

The frequency response of the proposed DBBPF is shown in figure 9.

Figure 9 can explain all our steps taken to have the dual-band bandpass frequency response of our proposed metamaterial filter. In this figure, we observe two different resonances that can define the two bandwidths located in the X-band each. For the first, 186.2 MHz wide bandwidth centred on the 9.89 GHz frequency, the filter has return losses of the order of -4.07 dB. For the other bandwidth centred on the 11.04 GHz frequency, the filter has return losses of the order of -11.22 dB. The significant gap observed between these two bandwidths contain a zero frequency of the order of 10.58 GHz, which has allowed us to have a considerable rejection band of the order of 1.03 GHz. This gap can be justified by the use of the two proposed metamaterial tapered resonators (SCI-SRR)<sub>2</sub> and (SCI-SRR)<sub>3</sub>. Figure 10 represents the cartography of the electric field on the DBBPF for the two different resonances.

In figure 10, we note that the electric field is confined in the coupling zone, more particularly in the microstrip arm connecting the two metamaterial resonators (SCI-SRRs)<sub>2</sub>

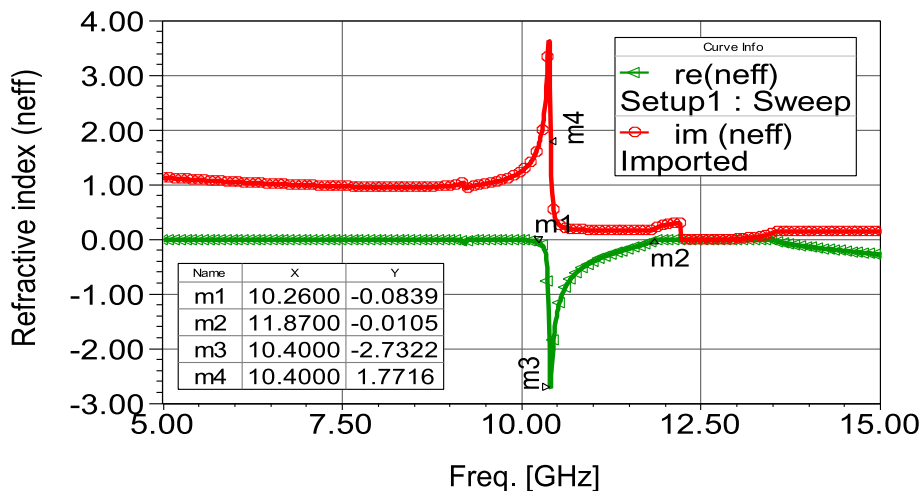


Figure 6. Refractive index of the (SCI-SRR)<sub>3</sub>; real and imaginary parts.

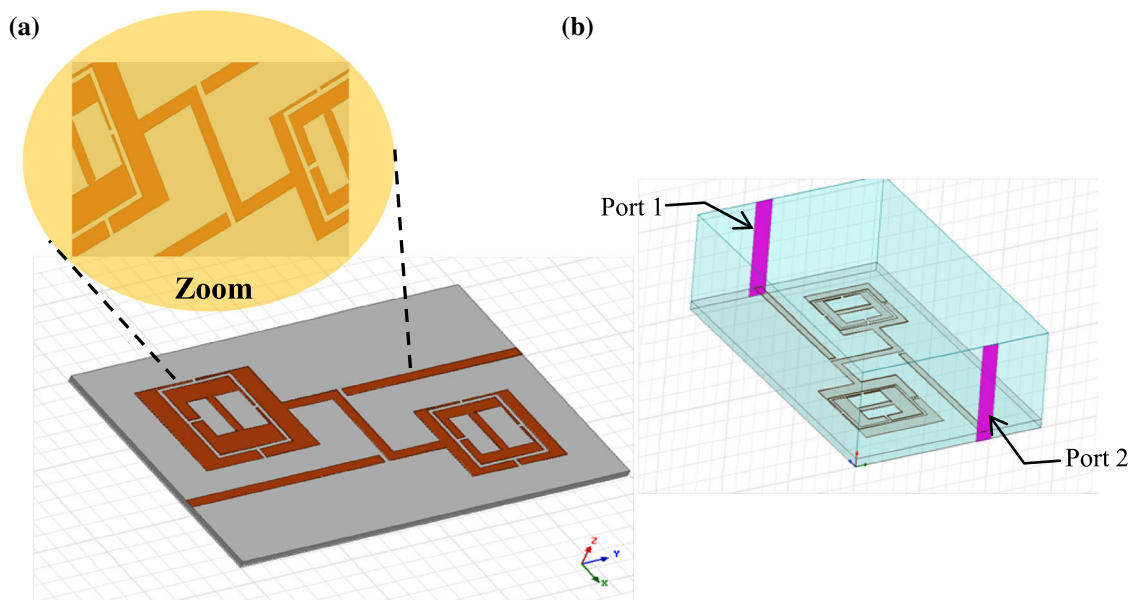


Figure 8. Proposed DBBPF. (a) 3-D view and (b) feeding ports.

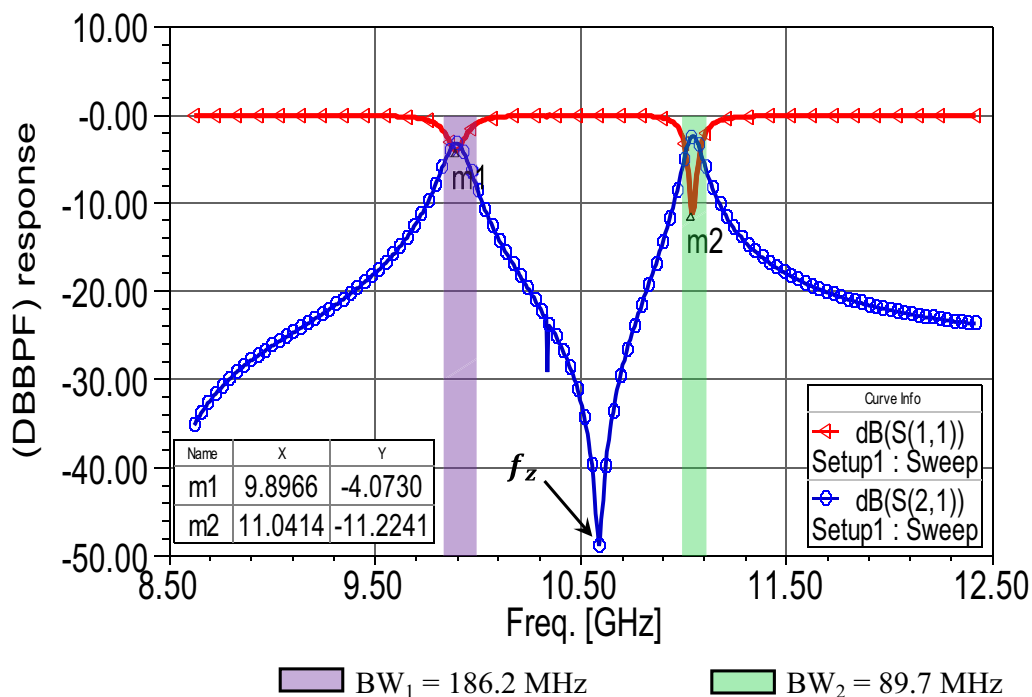
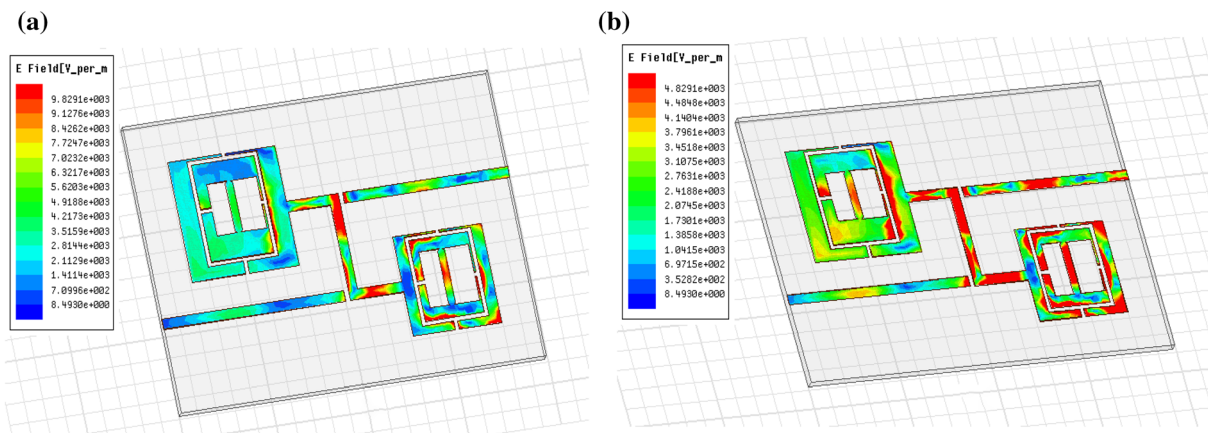


Figure 9. DBBPF response.

and (SCI-SRRs)<sub>3</sub>. At the first resonance of 8.89 GHz, we observe that the electric field is more condensed in the small resonator (SCI-SRR)<sub>2</sub>, while at the second resonance we can observe that it is a transfer of energy from this resonator to (SCI-SRRs)<sub>3</sub>, which corresponds to maximum electromagnetic power in the overall filter.

A comparison of our results for the performance of the new filter with other existing DBBPF in literature is summarized in table 2.

Table 2 gives the performance comparison results of the DBBPF proposed in this work and other DBBPFs in the references. Compared to its counterparts, our proposed filter



**Figure 10.** Mapping of the electric field on the DBBPF at resonance frequencies; (a)  $f_{01} = 8.89$  GHz and (b)  $f_{02} = 11.04$  GHz.

**Table 2.** Performance comparison of the designed filter with literature.

Reference	[26]	[27]	[28]	This work
Resonator structure	Parallel coupled line	Meander line	Single square	Tapered (SCI-SRR)
Centre frequency (GHz)	7.6/11.5	0.81/2.42	1.85/3.05	8.89/11.04
IL (dB)	0.6/0.92	1.4/2.2	2.72/3.21	2.68/2.61
RL (dB)	16.32/20	12 / 20	15/>15	4.07/11.22
Filter area (mm <sup>2</sup> )	18.4 × 9	51.85 × 11.11	80 × 30	39.6 × 27.7
Frequency band	C- and X-band	P- and S-band	L- and S-band	X-band
Applications	Modern communication systems	RFID applications	Sensor applications	Wireless communications

has a remarkable electrical quality that allows them to be used for wireless communications.

#### 4. Conclusions

In this paper, a dual-band bandpass microwave filter (DBBPF) is provided. This filter is inspired by a pair of tapered coupled interlinked metamaterial resonators SCI-SRRs; for the same asymmetric square shape of different sizes. The design of our DBBPF is based on the necessary electromagnetic coupling between the two chosen SCI-SRRs and the two microstrip lines for parallel feeding. The overall dimensions of our DBBPF are calculated according to the millimetre dimensions of the two proposed SCI-SRRs to have a frequency response in the X-band. The proposed tapered shape for our two metamaterial resonators, which are interconnected together by a conductive arm, contributed to the creation of the rejection band in the order of 1.03 GHz. The obtained results show that our designed filter, which is selective, meets our needs for X-band applications for two bandwidths of the order of 186.2 and 89.7 MHz, respectively.

#### Acknowledgements

We express our sincere thanks to the General Directorate of Scientific Research and Technological Development (DGRSDT) for their support in the development of this work.

#### References

- [1] Chen L, Li X and Wei F 2017 *J. RF Eng. Tel.* **71** 311
- [2] Reja A H and Ahmad S N 2015 *Adv. Intell. Syst. Comp.* **320** 179
- [3] Boutejdar A and Bennani S D 2017 *Adv. Electromagn.* **6** 18
- [4] Zhang S, Cheng J, Guo Y, Liu H and Liu F 2019 *Micro. Opt. Technol. Lett.* **61** 1
- [5] Chien Pheng E Z and Wong P W 2017 *Prog. Electromagn. Res.* **72** 141
- [6] Berka M, Mahdjoub Z and Hebali M 2018 *J. Electr. Eng.* **69** 311
- [7] Maragheh S, Dousti M, Dolatshahi M and Ghalamkari B 2019 *J. Electr. Commun. (AEÜ)* **111** 1
- [8] Veselago V G 1968 *Sov. Phys. Uspekhi.* **10** 509
- [9] Pasko W, Tralle I, Majchrowski K, Zieba P and Çoruh A 2018 *J. Mater. Sci.* **53** 2034



- [10] Navarroa R, Liard L and Sokoloff J 2019 *J. Appl. Phys.* **126** 1
- [11] Pandit S, Mohan A and Ray P 2019 *Appl. Phys. A* **125** 414
- [12] Feng T H and Han H P 2019 *J. Electron. Mater.* **48** 1252
- [13] Marquez R, Medina F and Raffi R 2002 *Phys. Rev. B* **65** 1
- [14] Altıntaş O, Aksoy M and Ünal E 2020 *Phys. E. Low Dimens. Syst. Nanostruct.* **116** 1
- [15] Dhar N, Rahman M A and Hossain M A 2020 *SN Appl. Sci.* **2** 1077
- [16] Berka M, Azzeddine H, Bendaoudi A, Mahdjoub Z and Rouabhi A Y 2021 *J. Electron. Mater.* **50** 4887
- [17] Mahfuz T A, Iqbal-Faruque M R, Jubaer M, Islam S and Tariqul-Islam M 2019 *Res. Phys.* **12** 2112
- [18] Rajkumar R and Kommuri U K 2018 *Wirel. Pers. Commun.* **101** 1075
- [19] Horestani A K, Fumeaux C, Al-Sarawi S F and Abbott D 2012 *IEEE Microw. Wirel Compon. Lett.* **22** 450
- [20] Bait-Suwailam M M, Almoneef T S and Saeed M 2020 *Prog. Electromagn. Res.* **95** 135
- [21] Nicolson A and Ross G 1970 *IEEE Trans. Instrum. Meas.* **19** 377
- [22] Weir W 1974 *IEEE* **62** 33
- [23] Luukkonen O, Maslovski S and Tretyakov S 2011 *IEEE Ant. Wirel. Propag. Lett.* **10** 1295
- [24] Hannan S, Islam M T and Almutairi A F 2020 *Sci. Rep.* **10** 10338
- [25] Panda A K, Mishra R K and Sahu S 2016 *Opt. Technol. Lett.* **58** 847
- [26] Lalbakhsh A, Alizadeh S M, Ghaderi A, Golestanifar A, Mohamadzade B, Jamshidi B M *et al* 2020 *Electronics* **9** 1770
- [27] Abdalla M, Choudhary D K and Chaudhary R K 2018 *J. Instrum.* **13** 1
- [28] Park E, Lim D and Lim S 2017 *Sens. J. (MDPI)* **17** 1